IL NUOVO CIMENTO **42 C** (2019) 225
DOI 10.1393/ncc/i2019-19225-4

COMMUNICATIONS: SIF Congress 2018

Ion transport and heating in simulations of plasma turbulence

F. PECORA(*)
Dipartimento di Fisica, Università della Calabria - Arcavacata di Rende (CS), Italy

received 30 April 2019

Summary. — The processes of particle diffusion and acceleration are currently being tackled worldwide because of their major implications in astrophysical and laboratory plasma physics. Despite the efforts of the whole community, a comprehensive theoretical description of such phenomena is still missing. In this work, a two-dimensional (2D) version of the Non-Linear Guiding Center (NLGC) theory is derived, in order to describe particle transport in some particular scenarios. The theory is validated with 2.5D kinetic simulations of plasma turbulence. Simulations parameters are chosen so that several scenarios can be described, going from the solar corona to the solar wind and the magnetosheath. Finally, the role of turbulence coherent structures on particle acceleration and energization is investigated. Current sheets are found to be of major importance in this scenario and that there is a scale-resonance interaction between the current sheet size and the particles' Larmor radii.

1. – Introduction

Understanding particle transport and acceleration phenomena could solve many of the currently puzzling problems of astrophysics. Particle acceleration is profoundly affected by turbulence, one example is the solar corona where plasma gets heated from explosive events [1]. In the same way, understanding diffusion in the interplanetary medium [2, 3] could tell whether energetic particles coming from a flare or a coronal mass ejection would hit a satellite, an astronaut or Earth. Coming down to Earth, a major problem for laboratory plasmas is confinement. A comprehensive description of the effects of turbulence on particle motion [4, 5] and acceleration [6] is needed in order to advance toward plasma fusion [7] and clean energy sources [8]. Charged particle motion in all these systems is deeply affected by the presence of turbulence. Particles do not only gyrate along the magnetic field lines, but they also spread in the plane perpendicular to the mean magnetic field [9-11]. Because of the turbulent nature of the fields scattering

(*) E-mail: francesco.pecora@unical.it

the particles, the analytical treatment is challenging and a statistical approach becomes appropriate [12, 13]. A fundamental quantity used to describe diffusion is the diffusion coefficient. In the case in which the motion along the mean field is decoupled from that in the perpendicular plane, also the coefficients are independent and can be calculated separately [13, 14]. In this scenario, the non-linear guiding centre (NLGC) theory [15] is able to accurately evaluate the diffusion coefficients for three-dimensional (3D) systems. Despite a more realistic description, 3D systems are much more computationally expensive with respect to 2D ones. However, 2D scenarios are useful when the system is embedded in a strong magnetic field. Previous studies have shown that, when a mean magnetic field is present, turbulence becomes anisotropic and the typical pattern of current sheets and reconnecting magnetic islands mainly develops in the plane perpendicular to the main field, while the structures are elongated in the parallel direction [16-18]. Due to this anisotropy, also magnetic field topology modification, and eventually energy exchange with particles, are mainly effective in the perpendicular plane [19-24]. Particle acceleration and energization are currently believed to be primarily due to magnetic reconnection [25, 26]. The magnetic field topology changes are detectable as explosive events, such as flares [27, 28] and coronal mass ejections [29], which release very quickly large amounts of energy stored in the field to particles. In this work, the approach used to tackle these phenomena is through self-consistent 2.5D simulations of plasma turbulence. In this approximation, the 3D fields depend on 2 spatial coordinates, granting a reduction of computational costs, with respect to a full 3D description, while being able to describe systems with a guiding magnetic field with almost the same accuracy. The realistic texture of turbulence that comes from the simulation is a good environment where to study particle diffusion. Moreover, to look at particle acceleration and energization, the self-consistent treatment is mandatory. It is through the feedback between fields and particles that these phenomena can produce more realistic effects.

This work is organized as follows: in sect. **2**, the model used to carry on the simulations is presented; sect. **3** contains the results about particle diffusion and sect. **4** shows how particles change their velocity through their journey. Finally, a brief discussion on the results is given.

2. – Simulation overview

The continuous feedback between particles and fields in low collisional plasmas is described through the Vlasov-Maxwell set of equations (1)

$$\dot{\mathbf{x}} = \mathbf{v}, \tag{1a}$$

$$\dot{\mathbf{v}} = \mathbf{E} + \mathbf{v} \times \mathbf{B}, \tag{1b}$$

$$\frac{\partial \mathbf{B}}{\partial t} = -\boldsymbol{\nabla} \times \mathbf{E}, \tag{1c}$$

$$\mathbf{E} = -(\mathbf{u} \times \mathbf{B}) + \frac{1}{n}\mathbf{j} \times \mathbf{B} - \frac{1}{n}\boldsymbol{\nabla} P_e + \eta \mathbf{j}, \tag{1d}$$

where $\mathbf{x}$ is the position of the particle and $\mathbf{v}$ its velocity. $\mathbf{E}$ and $\mathbf{B}$ are the electric and magnetic fields respectively. Let $f(\mathbf{x}, \mathbf{v}, t)$ be the ion velocity distribution function, so $n = \int f \, \mathrm{d}\mathbf{v}$ is the ion number density, $\mathbf{u} = (1/n) \int \mathbf{v} \, f \, \mathrm{d}\mathbf{v}$ is the bulk flow speed. $\mathbf{j} = \boldsymbol{\nabla} \times \mathbf{B}$ is the current density, the electron pressure term is modeled with an adiabatic equation $P_e = \beta n^\gamma$ and $\eta = 6 \cdot 10^{-3}$ introduces small-scale dissipation to prevent numerical noise from building up. In the code, distances are normalized to the ion inertial

length, $d_i = c/\omega_{pi}$, where c is the speed of light and ω_{pi} is the ion plasma frequency. Time is normalized to the inverse of ion cyclotron frequency Ω_{ci}^{-1}. Velocities are normalized to the Alfvén speed, $c_A = c\Omega_{ci}/\omega_{pi}$. Simulations were performed with a hybrid-PIC code [30]. The hybrid choice allows the kinetic description of ions while electrons are treated as a massless fluid that grants the pressure term described above. The loss of small-scale description is compensated by shorter computational times. The Particle-In-Cell (PIC) technique is widely used when a self-consistent approach is needed, *e.g.*, when treating energy exchange between fields and particles. The PIC method is based on the sampling of the particle velocity distribution function (VDF). Equations (1) are solved for the so-called "macro-particle", that are the VDF slices mentioned above. Because of this partitioning, PIC codes tend to be noisy if the macro-particles are chosen as wide bins of the VDF. The domain used is $(128 \times 128)d_i^2$, discretized with 512×512 cells and periodic boundary conditions. In order to reduce the implicit noise coming from the PIC technique, there are 1500 particles per cell for a total of more than 10^8 total particles. Simulations were carried out with three different values of the plasma β, the ratio between the thermal and the magnetic pressures, to be able to describe very different environments, such as solar corona ($\beta = 0.1$), solar wind ($\beta = 0.5$) and magnetosheath ($\beta = 5$). All the simulations have the same initial conditions of uniform density and temperature and the starting VDFs are Maxwellian. Turbulence is initiated imposing large-scale random fluctuations, in the plane perpendicular to the guiding field, for the magnetic field and the ion bulk velocity field. The amplitude of the fluctuations is $\delta B/B_0 \sim 0.3$. When using the 2.5D geometry approximation, it is handy to set the guiding field along one axis, *e.g.*, the z-direction, and the magnetic field in the perpendicular plane is $B_\perp = \boldsymbol{\nabla} a_z \times \hat{z}$, where a_z is the vector potential. The current density in the axial direction is $j_z = (\boldsymbol{\nabla} \times B_\perp) \cdot \hat{z} = -\nabla^2 a_z$. After initial free evolution, the system is forced to remain in a state of fully developed turbulence by "freezing" the amplitudes and the phases of the in-plane magnetic field modes ($1 \leq m \leq 4$) as described in [31]. The time at which the system reaches the state of fully developed turbulence is individuated when non-linearity (or j^2) reaches a peak, and it happens at roughly $t^* \sim 50\Omega_{ci}^{-1}$.

Figure 1 shows the shaded contour of the current density j_z with isocontour of magnetic potential a_z at two different times. On the left, the system is shown during its

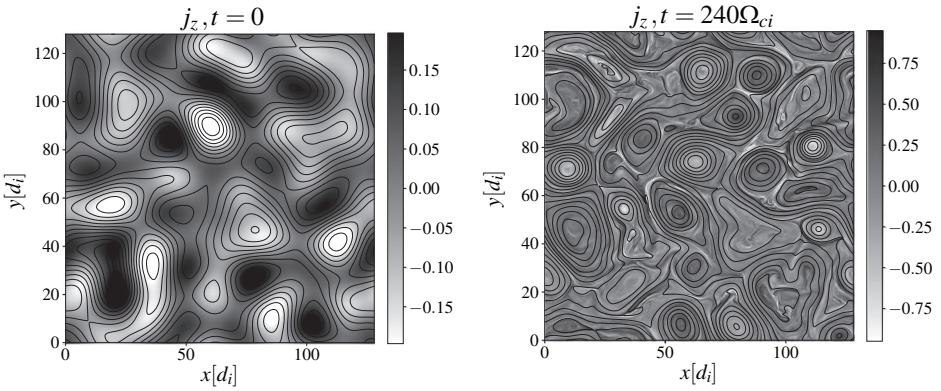

Fig. 1. – Shaded contour of the current density with magnetic potential isocontour. On the left the initial state is shown whereas, on the right, a state of fully developed turbulence is reported. The development of smaller island and intense current sheets, as expected from MHD turbulence, is evident.

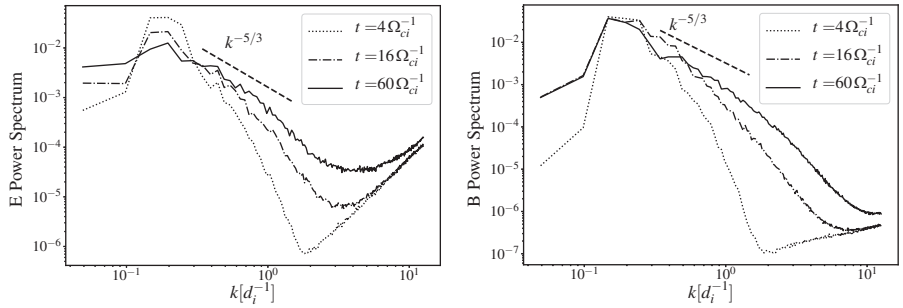

Fig. 2. – Power density spectra of electric (left) and magnetic (right) fields. The spectra show the cascading behaviour of turbulence for which energy flows from large to small scales producing the well-known slope $k^{-5/3}$ in the inertial range. After a certain time, the state of fully developed turbulence is reached and the spectra become stationary.

initial state, when only a few big vortices are present. The intensity of the current is not developed yet and all structures appear to be mild and smooth. On the other hand, when turbulence is fully developed, a number of increasingly small and intense structures appear. The effect of turbulence is to fragment the bigger vortices, at the injection scale, into smaller and sharper structures all the way down to the dissipative scale through the inertial range. In the right panel we see this latter scenario, where the volume is filled with magnetic islands of different sizes and intense current sheet appear in between them, possibly due to reconnection mechanisms [32, 33]. The classical picture of MHD turbulence can be seen more directly when computing the power spectra of electric and magnetic fields. These spectra are shown in fig. 2. It is clearly visible how small-scale structures are developed in time: energy flows from large scales (small k's) and populates small scales (big k's). The spectra become stationary after the non-linearity peak is reached. The slope of the spectra in the inertial range is that expected from *in situ* measurements [34]. The electric field spectrum rising at scales smaller than the ion skin depth is due to numerical noise.

3. – Diffusion

Both the visual appearance of turbulence and the spectra suggest that the described system can be related quite closely to actual astrophysical scenarios where ion behaviour can be studied. This section and the following one are, hence, focused on particles. All analyses were done during the steady state of fully developed turbulence, namely $50 < t\Omega_{ci} < 250$. Of all the $>10^8$ particles, position and velocity data have been stored for $>10^5$ particles. The position of each particle during the simulation is used to compute the displacement in the perpendicular (x-y) plane. This quantity, defined as $\Delta s^2 = \Delta x^2 + \Delta y^2$, where $\Delta x = x(t_0 + \tau) - x(t_0)$ with x being a particle's position along the x-direction, is fundamental when treating diffusion. It is well known [35] that, when diffusive motion is achieved, the mean squared displacement can be described as

$$\langle \Delta s^2 \rangle = 2D\tau, \tag{2}$$

where the averaging operation $\langle \dots \rangle$ is made over an ensemble of particles, D is the perpendicular diffusion coefficient and τ is the time interval over which the displacement

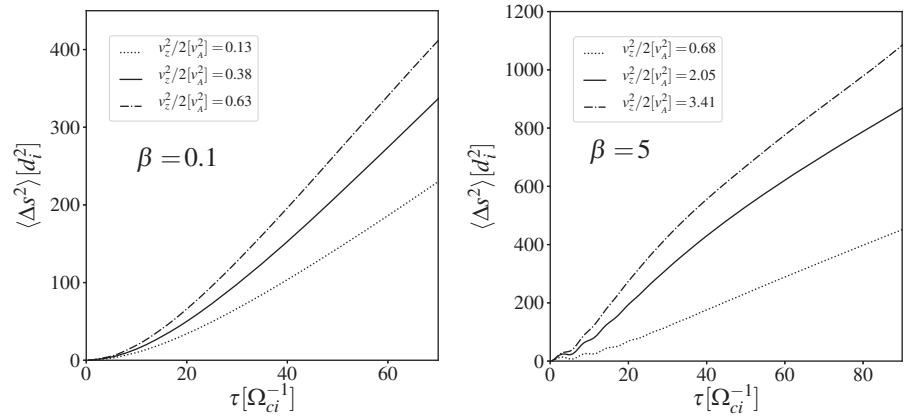

Fig. 3. – Mean squared displacement for particles divided in energy bins and for different β values.

is calculated. If this quantity is measured for particles moving in turbulent fields, it can be seen that, after a transient time, this behaviour is reached. In these simulations, particles have been divided in parallel energy ($v_z^2/2$) groups to see also their influence on the diffusion coefficient.

Figure 3 shows the mean squared displacement as a function of the elapsed time interval τ for ions selected on their parallel energy. What can be noticed is that the larger the energy, the larger the perpendicular displacement, whichever β. Currently, one of the best theories that describes the diffusion coefficient is the NLGC theory in its simplest form [15]. This theory is widely used and many upgrades and different versions have been proposed [11, 36, 37]. To describe particles in a 2.5D scenario an alternative version was needed because the theory itself was born to describe 3D environments. The starting point is the Taylor-Green-Kubo formulation [12, 38, 39] that enables writing the diffusion coefficient in the x-direction in terms of the particles' velocity and magnetic field, namely

$$D_{xx} = \int_0^\infty \langle v_z(0) B_x(\mathbf{x}(0), 0)\, v_z(\tau) B_x(\mathbf{x}(\tau), \tau) \rangle \mathrm{d}\tau.$$

Through some manipulation, explicitly expressed in [40], the final relation for the perpendicular diffusion coefficient reads

$$D^2 \sim \frac{v_z^2}{B_0^2} \int \frac{S(\mathbf{k})}{k^2} \mathrm{d}\mathbf{k}, \tag{3}$$

where v_z is the particle velocity in the axial direction, that is the one where the guiding field B_0 points, $S(\mathbf{k})$ is the power spectral density of the magnetic field and $\mathbf{k}$ is the wave vector. By fitting the mean squared displacements shown in fig. 3 when the linear trend is achieved, an experimental estimate of the diffusion coefficient can be obtained. The theoretical expectation is, instead, calculated via eq. (3). A comparison of the diffusion coefficient values obtained directly from the simulations and from the theoretical approach is given in fig. 4.

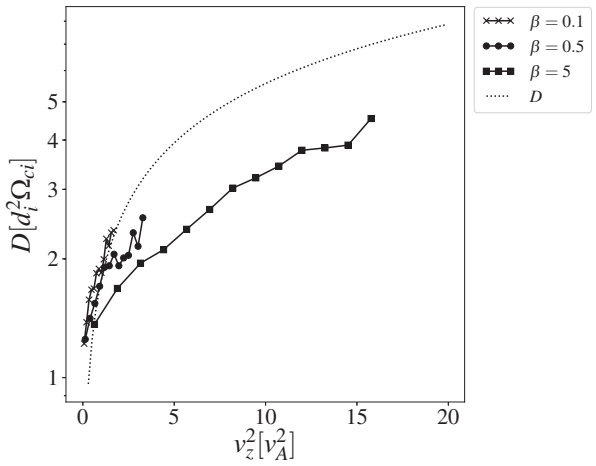

Fig. 4. – Comparison of experimental (symbols) and theoretical (black dotted line) diffusion coefficient.

From fig. 4 it can be noticed that the theory describes rather well the diffusive behaviour of particles in the low β regime, while there is some deviation when considering large β plasmas, though the trend is the same. This difference can be due to the fact that, when β is low, particles are more magnetized and the guiding centre approximation can hold better. In any β scenario, the theory, as expected from the existing literature [9,15], shows that diffusivity depends on particles' energy. There is no β dependence since this parameter was changed by changing particles' temperature, resulting in particles having larger energies in the high β plasma, and hence diffusing more, and particles with smaller energies in the low β case, diffusing less.

4. – Particle heating

Particle acceleration and energization mechanisms are yet to be completely understood, especially when they are tied to diffusion properties. In this last section the causes of variations in particles' velocity and how this is linked to turbulence features are

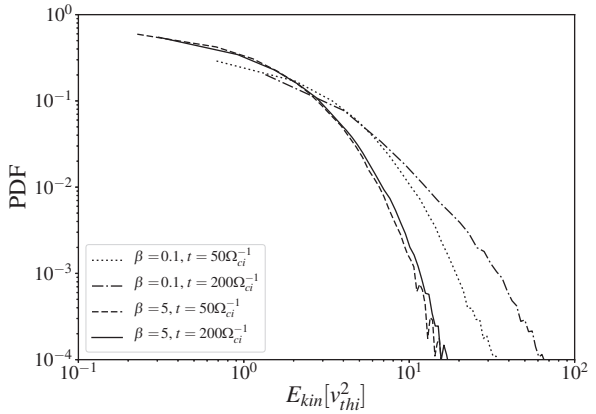

Fig. 5. – Ion kinetic energy PDFs at initial and final times and for the two extreme values of β.

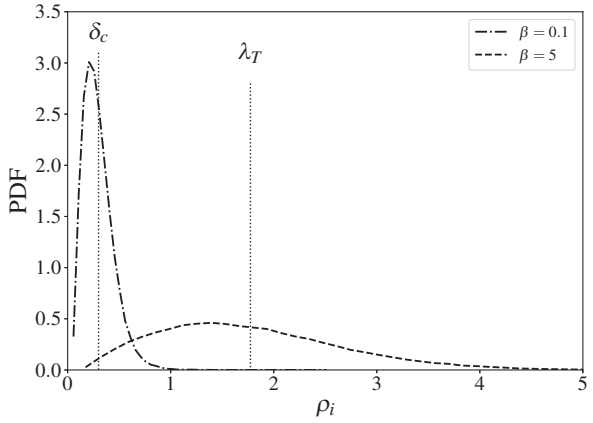

Fig. 6. – Ions Larmor radii PDF's for low and high β plasmas. In the plot, the current sheets core average width δ_c and the Taylor microscale λ_T are also indicated.

investigated. From Lagrangian velocity it is possible to evaluate acceleration and energy of each particle during the whole simulation.

The probability density functions (PDF) of ions' energy, shown in fig. 5, evidence different behaviours depending on the plasma β. In the solar-corona–like scenario, the tail developed at later times by energy PDF indicates that particles have been through considerable heating processes. On the other hand, in the magnetosheath-like scenario, the PDF seems to be unchanged, suggesting that particles are less sensitive to acceleration and energisation phenomena. It is interesting to find a link between particle acceleration and turbulence characteristic scales. One definition for a scale is that called Taylor microscale, namely

$$\lambda_T^2 = \frac{\delta b_\perp^2}{\langle j^2 \rangle},$$

where $\delta b_\perp$ are the magnetic field fluctuations in the perpendicular plane. This scale represents roughly the size of the largest dissipative structures. Another interesting scale is the average size of current sheets' cores, δ_c, namely the width of the most intense region of the current sheets. On the one hand, a scale to which particles can be associated is the size of their gyrating motion, namely their Larmor radius. By spotting the two turbulence scales defined above over the PDF of ions Larmor radii ρ_i, it is immediately noticeable that particles in the low β plasma have the "right" size to actively interact with current sheets, as shown in fig. 6. On the other hand, particles moving in the high β plasma, have gyration radii large enough to avoid current sheets. This kind of scale-resonant interaction might explain why particles are heated in one scenario and not in the other.

5. – Conclusion

In this work the topics of diffusion and acceleration processes acting on ions in turbulent plasma scenarios have been tackled. The different scenarios, from solar corona to solar wind and Earth's magnetoshphere, have been simulated using a self-consistent

hybrid-PIC code. To reduce the computational cost, the geometry was simplified to 2.5 dimensions. This geometry finds applications in structures with a strong mean magnetic field, such as coronal loops or plasma fusion machines. Generally, this approximation is valid when treating any kind of anisotropic turbulence [16, 41, 42]. The PIC approach used is of fundamental importance when wave particle interactions have to be taken into account. Current density 2D maps showed that the simulated turbulent environment develops small-scale structures, as magnetic islands and current sheets, and magnetic and electric field power spectra displayed common features also found in *in situ* measurements, such as Kolmogorov's inertial range power law prediction $k^{-5/3}$. Ion motion in turbulence is very erratic [31, 43], but it can be statistically described, for sufficiently long time intervals, with diffusion theory. Among all the currently developed theories, the NLGC one seems to be one of the most accurate in predicting the diffusion coefficient. In this work, a "reduced" version, derived in [40], was presented and it is able to describe diffusive motion in 2D scenarios. Diffusion seems to be affected by particles energy. On the contrary, acceleration and heating processes seem to strongly depend on this parameter as the PDFs of particles energy show. In the high β system, the energy is a stochastic variable and it does not evolve in time. On the other hand, in the low β plasma, the energy is stochastic at the beginning of the simulation but it develops a power law tail at later times. A local resonance was found between particles and turbulence properties. When ions have Larmor radii of the order of the width of currents sheets, they experience local coherent energization resulting in global heating. In the high β plasma, most of the ions have gyration radii larger than the Taylor length, meaning that, in this case, particles can barely interact with current sheets. The results of this work have been published in a more detailed version in [40].

* * *

This work is partly supported by the International Space Science Institute (ISSI) in the framework of International Team 405 entitled "Current Sheets, Turbulence, Structures and Particle Acceleration in the Heliosphere".

REFERENCES

[1] Temmer M., Veronig A., Kontar E., Krucker S. and Vršnak B., *Astrophys. J.*, **712** (2010) 1410.
[2] Ruffolo D., Matthaeus W. H. and Chuychai P., *Astrophys. J.*, **597** (2003) L169.
[3] Ruffolo D., Matthaeus W. H. and Chuychai P., *Astrophys. J.*, **614** (2004) 420.
[4] Taylor J. B. and McNamara B., *Phys. Fluids*, **14** (1971) 1492.
[5] Hauff T., Pueschel M. J., Dannert T. and Jenko F., *Phys. Rev. Lett.*, **102** (2009) 075004.
[6] Petrosian V., *Space Sci. Rev.*, **173** (2012) 535.
[7] Li J., Guo H., Wan B., Gong X., Liang Y., Xu G., Gan K., Hu J., Wang H., Wang L. *et al.*, *Nature Phys.*, **9** (2013) 817.
[8] Hora H., Miley G. H., Ghoranneviss M., Malekynia B., Azizi N. and He X.-T., *Energy Environ. Sci.*, **3** (2010) 478.
[9] Jokipii J. and Parker E., *Astrophys. J.*, **155** (1969) 777.
[10] Chandran B. D. G., Li B., Rogers B. N., Quataert E. and Germaschewski K., *Astrophys. J.*, **720** (2010) 503.
[11] Ruffolo D., Pianpanit T., Matthaeus W. H. and Chuychai P., *Astrophys. J. Lett.*, **747** (2012) L34.
[12] Green M. S., *J. Chem. Phys.*, **19** (1951) 1036.

[13] Jokipii J., *Astrophys. J.*, **146** (1966) 480.
[14] Subedi P., Sonsrettee W., Blasi P., Ruffolo D., Matthaeus W., Montgomery D., Chuychai P., Dmitruk P., Wan M., Parashar T. and Chhiber R., *Astrophys. J.*, **837** (2017) 140.
[15] Matthaeus W., Qin G., Bieber J. and Zank G., *Astrophys. J. Lett.*, **590** (2003) L53.
[16] Matthaeus W. H. and Lamkin S. L., *Phys. Fluids*, **29** (1986) 2513.
[17] Greco A., Matthaeus W. H., Servidio S., Chuychai P. and Dmitruk P., *Astrophys. J.*, **691** (2009) L111.
[18] Servidio S., Greco A., Matthaeus W. H., Osman K. T. and Dmitruk P., *J. Geophys. Res.*, **116** (2011) A09102.
[19] Parker E. N., *J. Geophys. Res.*, **62** (1957) 509.
[20] Matthaeus W. H., Ambrosiano J. J. and Goldstein M. L., *Phys. Rev. Lett.*, **53** (1984) 1449.
[21] Ambrosiano J., Matthaeus W. H., Goldstein M. L. and Plante D., *J. Geophys. Res.*, **93** (1988) 14383.
[22] Servidio S., Matthaeus W. H., Shay M. A., Cassak P. A. and Dmitruk P., *Phys. Rev. Lett.*, **102** (2009) 115003.
[23] Servidio S., Valentini F., Perrone D., Greco A., Califano F., Matthaeus W. H. and Veltri P., *J. Plasma Phys.*, **81** (2015) 325810107.
[24] Bruno R. and Carbone V. (Editors), *Turbulence in the Solar Wind*, in *Lecture Notes in Physics*, Vol. **928** (Springer Verlag, Berlin) 2016.
[25] Servidio S., Dmitruk P., Greco A., Wan M., Donato S., Cassak P., Shay M., Carbone V. and Matthaeus W., *Nonlin. Process. Geophys.*, **18** (2011) 675.
[26] Zank G. P., le Roux J. A., Webb G. M., Dosch A. and Khabarova O., *Astrophys. J.*, **797** (2014) 28.
[27] Cargill P. J., Vlahos L., Turkmani R., Galsgaard K. and Isliker H., *Space Sci. Rev.*, **124** (2006) 249.
[28] Cargill P. J., Vlahos L., Baumann G., Drake J. F. and Nordlund Å., *Space Sci. Rev.*, **173** (2012) 223.
[29] Gosling J. T., *AIP Conf. Proc.*, **1216** (2010) 188.
[30] Franci L., Landi S., Matteini L., Verdini A. and Hellinger P., *Astrophys. J.*, **812** (2015) 21.
[31] Servidio S., Haynes C. T., Matthaeus W. H., Burgess D., Carbone V. and Veltri P., *Phys. Rev. Lett.*, **117** (2016) 095101.
[32] Matthaeus W. H. and Montgomery D., *Ann. New York Acad. Sci.*, **357** (1980) 203.
[33] Servidio S., Valentini F., Perrone D., Greco A., Califano F., Matthaeus W. and Veltri P., *J. Plasma Phys.*, **81** (2015) 325810107.
[34] Bale S. D., Kellogg P. J., Mozer F. S., Horbury T. S. and Reme H., *Phys. Rev. Lett.*, **94** (2005) 215002.
[35] Chandrasekhar S., *Rev. Mod. Phys.*, **15** (1943) 1.
[36] Shalchi A., Bieber J. and Matthaeus W., *Astrophys. J.*, **615** (2004) 805.
[37] Bieber J. W., Matthaeus W. H., Shalchi A. and Qin G., *Geophys. Res. Lett.*, **31** (2004) L10805.
[38] Taylor G. I., *Proc. London Math. Soc.*, **20** (1922) 196.
[39] Kubo R., *J. Phys. Soc. Jpn.*, **12** (1957) 570.
[40] Pecora F., Servidio S., Greco A., Matthaeus W. H., Burgess D., Haynes C. T., Carbone V. and Veltri P., *J. Plasma Phys.*, **84** (2018) 725840601.
[41] Shebalin J. V., Matthaeus W. H. and Montgomery D., *J. Plasma Phys.*, **29** (1983) 525.
[42] Dmitruk P., Matthaeus W. H. and Seenu N., *Astrophys. J.*, **617** (2004) 667.
[43] Rappazzo A., Matthaeus W., Ruffolo D., Velli M. and Servidio S., *Astrophys. J.*, **844** (2017) 87.